Electronic Supplementary Material (ESI) for Dalton Transactions.
This journal is © The Royal Society of Chemistry 2024

Supporting Information

Utilization of a trinuclear Cu-pyrazolate inorganic motif to build multifunctional MOFs.

Sayan Saha[§], Sohel Aktar[§], Subhendu Pramanik, Sukhen Bala, and Raju Mondal*

AUTHOR INFORMATION

Corresponding Author

Raju Mondal − School of Chemical Sciences, Indian Association for the Cultivation of Science, 2A &2B Raja S. C. Mullick Road, Jadavpur, Kolkata 700 032, India;
orcid.org/0000-0002-9013-7259;
Email: icrm@iacs.res.in

Authors

Sayan Saha, Sohel Aktar, Subhnedu Pramanik, Sukhen Bala
School of Chemical Sciences, Indian Association for the Cultivation of Science, 2A &2B Raja S. C. Mullick Road, Jadavpur, Kolkata 700 032, India

§: Contributed equally as a first author.

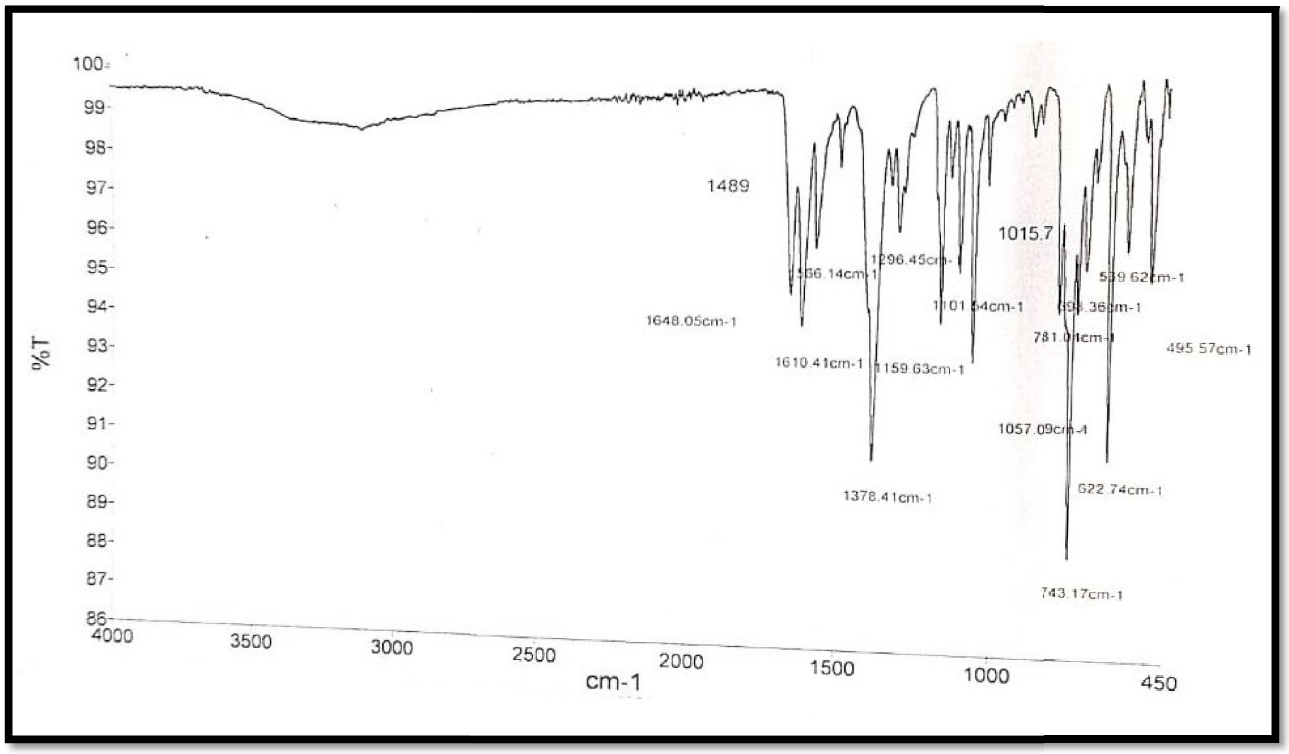

Figure S1 : IR Spectra of MOF-1.

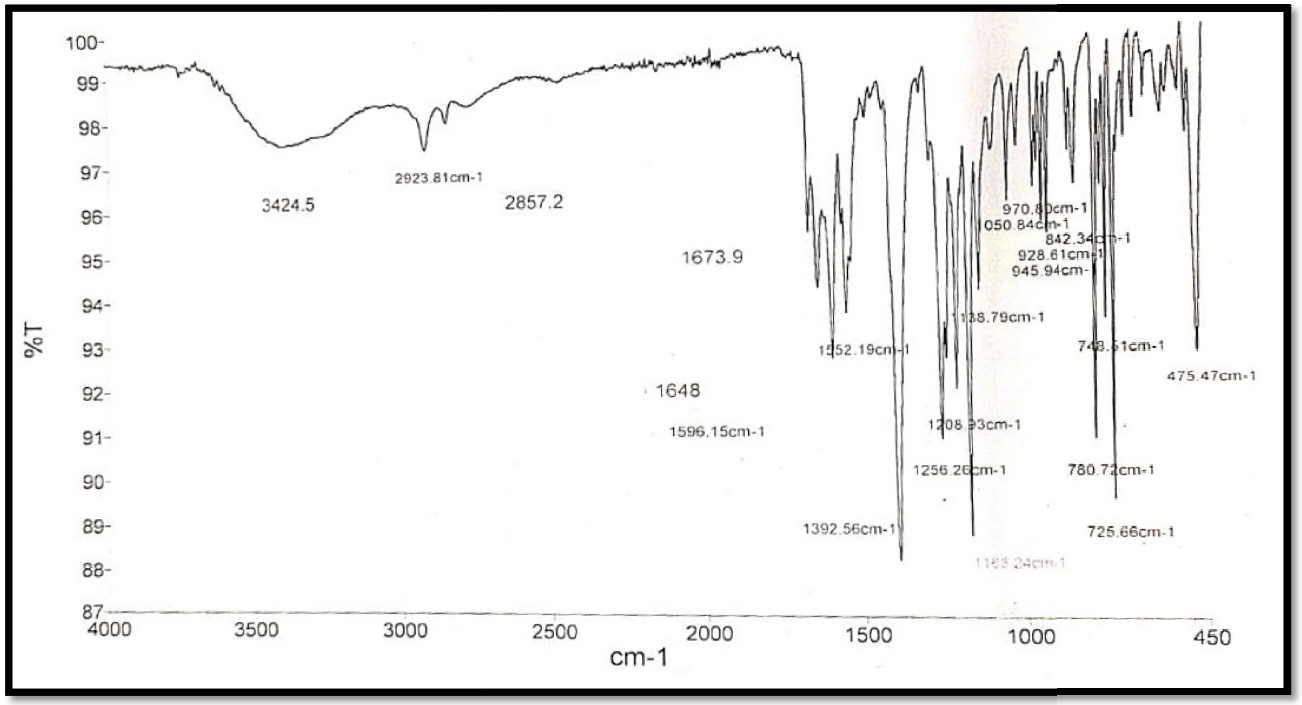

Figure S2 : IR Spectra of MOF-2.

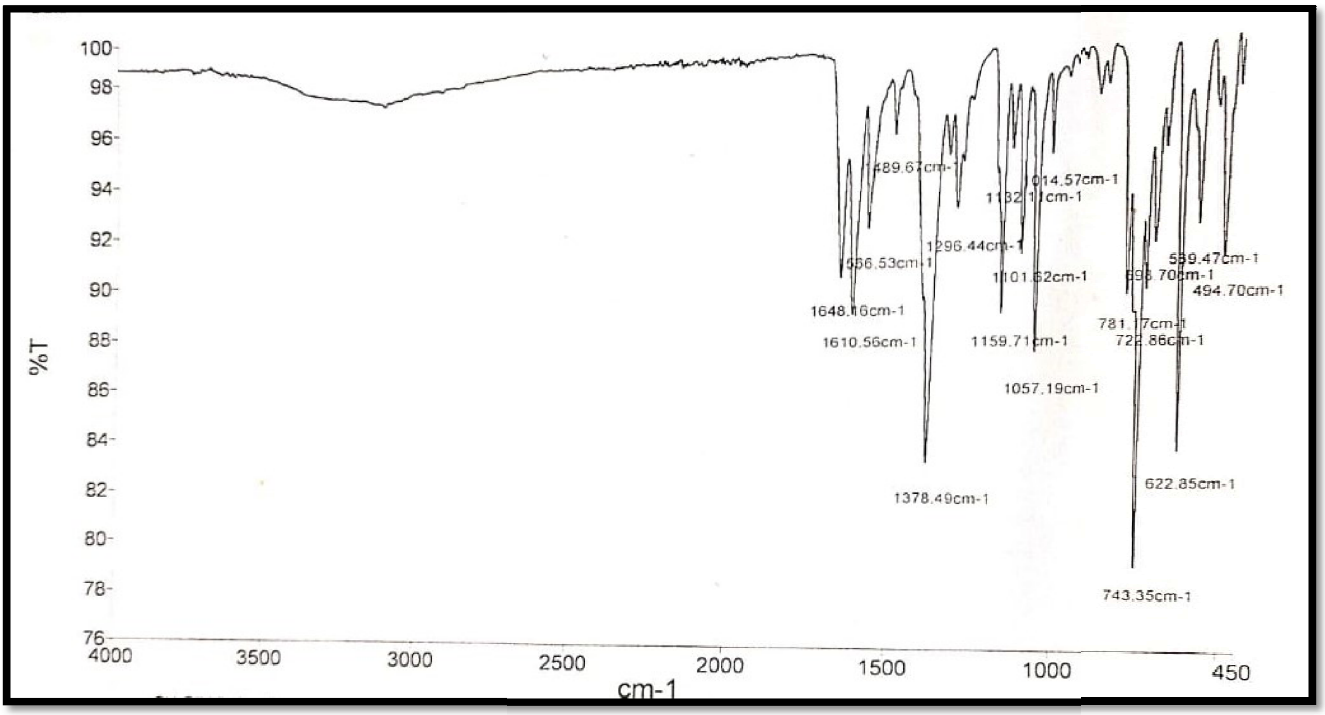

Figure S3 : IR Spectra of MOF-3.

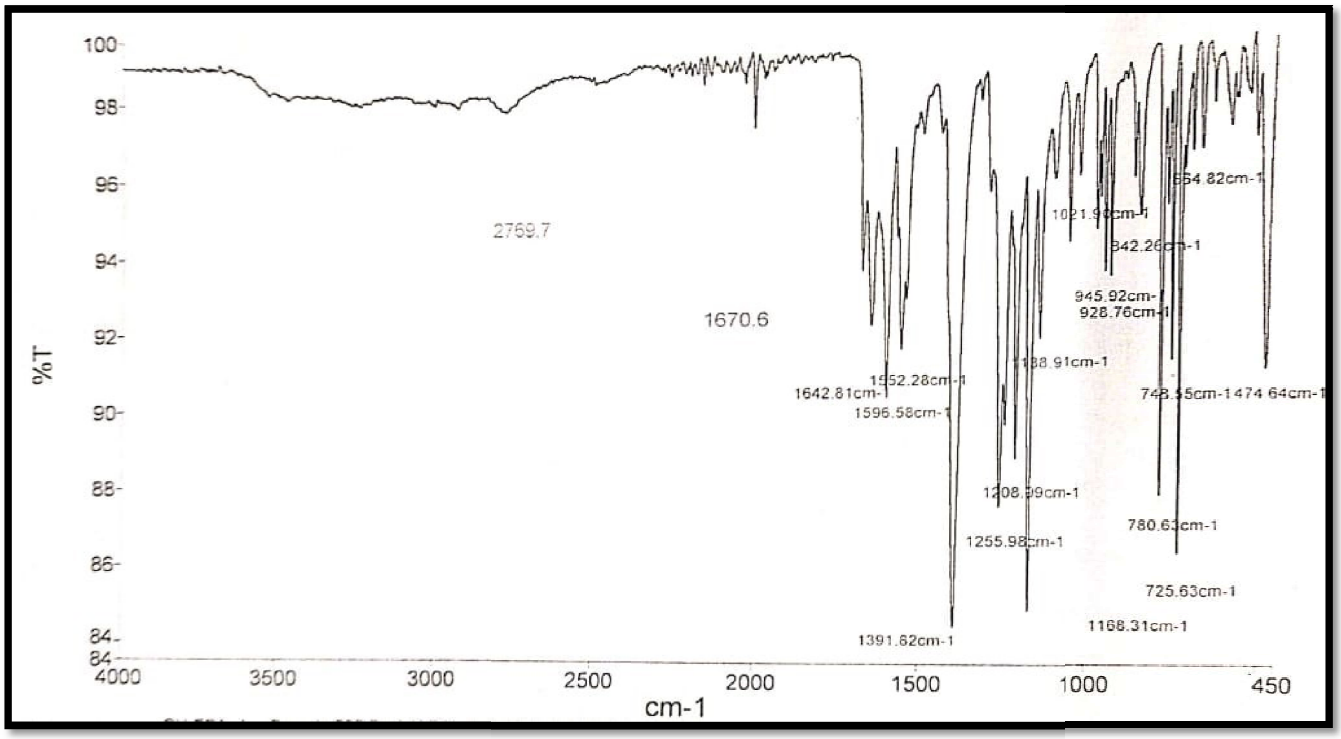

Figure S4 : IR Spectra of MOF-4.

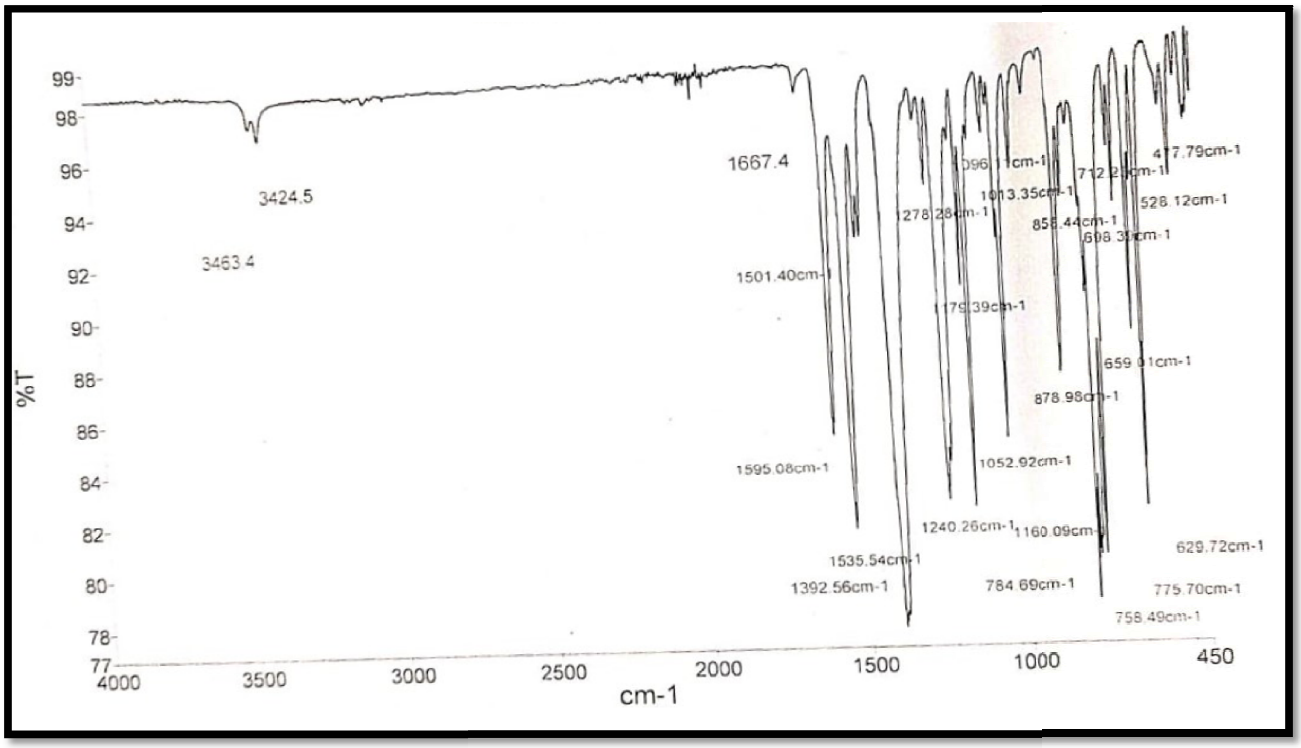

Figure S5 : IR Spectra of MOF-5.

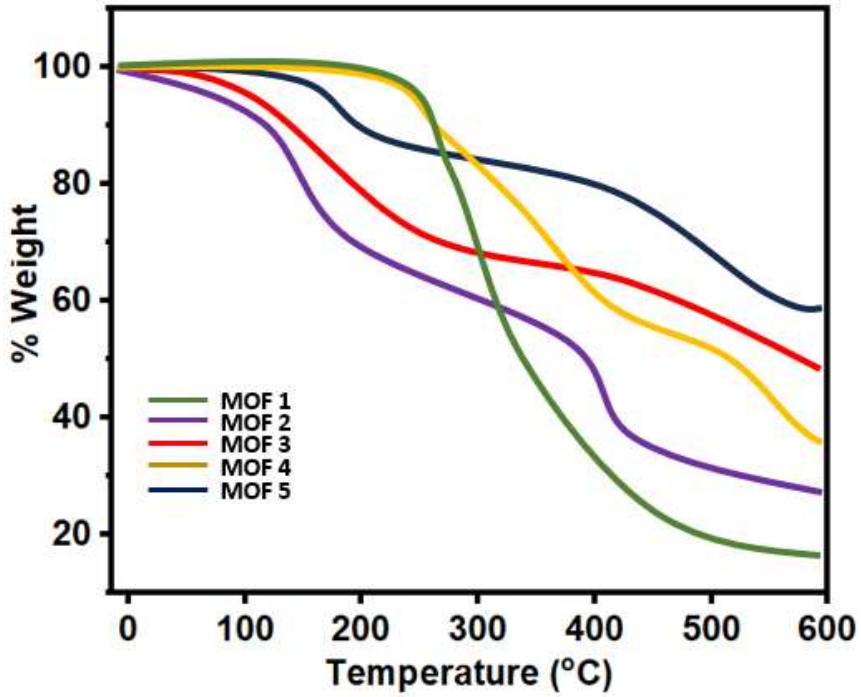

Figure S6: Thermogravimetric analysis of MOF 1-5 from RT to 600ºC.

Exploring the TGA of the MOFs

It was obviously necessary to check the thermal stability of both MOFs before the fabrication of electrical devices with these materials. Therefore, thermogravimetric analyses (TGA) for all the MOFs were performed (Fig. S6).The TGA of **MOFs 1-5** was performed in platinum crucible at a rate of 10 ºC per minute under nitrogenous atmosphere within the range of 0-600ºC.

All the MOFs showed considerable thermal stability. **MOF 1** shows a sharp fall of weight loss in the higher temperature range due to release of trapped Solvent molecule. PLATON study also confirms about Total Potential Solvent Area Vol. 151.4 $Å^3$. The next, the weight loss continue as a steady state manner in the higher temperature range is due to the decomposition of the compound. In the case of **MOF 2** the initially a gradual weight lossupto 100 °C is due to the loss of water molecules per asymmetric unit. Now there is a sharp fall starts around 140°C due to the trapped Acetate molecules present as counter anion in the lattice goes for the decarboxylation reaction. PLATON study also confirms about Total Potential Solvent Area Vol. for **MOF 2** is around 104.3$Å^3$In case of **MOF 3**there is a gradual decrease of weight loss was observed upto 200°CPLATON calculations conclude Unit cell Contains NO Residual Solvent Accessible Void. So, the reason maybe that decarboxylation of the bonded carboxylic acid was started. Which continues as a result it ruptures over all construction of the MOF. In case of **MOF 4**Now, there is a monodentate $SO4^{2-}$ ions bridged with Cu-Pyz SBU unit. According to Fajans' rules, metal coordinated sulphate evolves SO_3 gas due to cleavage of the metal–oxygen bond at higher temperature. We observed almost 60 % weight loss in the temperature range of 300°– 400 °C due to the aforesaid phenomenon The next part of weight loss beyond 400 °C is because of gradual thermal disintegration of the interpenetrating network of **MOF 4**. The networks of all the MOFs show extraordinary thermal stability, thereby enabling us to use them for catalyst purpose.

Table S1: Crystallographic data and refinement parameters of MOFs 1-5.

	MOF-1	MOF-2	MOF-3	MOF-4	MOF-5
Emperical formula	$C_{92}H_{92}Cu_{12}N_{24}O_{34}$	$C_{28.90}H_{22.80}Cu_3F_6N_7O_{6.40}$	$C_{17}H_{20}Cu_3N_6O_5$	$C_{42}H_{45}Cu_6N_{20}O_{12}S$	$C_{31}H_{38}Cu_3N_9O_{11}S$
Crystal system	monoclinic	triclinic	triclinic	triclinic	triclinic
Formula wt	2840.37	875.16	579.01	1435.28	935.38
Space group	P2/c	P ī	P ī	P ī	P ī
a/Å	17.760(12)	9.4907(10)	9.001(5)	11.5378(11)	9.221(2)
b/Å	9.823(7)	13.7197(14)	9.519(5)	15.7422(13)	12.471(4)
c/Å	17.162(12)	16.1356(17)	11.394(6)	16.9487(16)	17.304(5)
α/°	90	114.378(4)	88.919(12)	107.464(3)	77.215(8)
β/°	116.558(12)	92.674(4)	85.325(12)	102.375(3)	88.784(7)
γ/°	90	107.127(4)	86.622(12)	96.080(3)	78.935(8)
V/Å^3	2678(3)	1794.4(3)	971.3(6)	2820.0(4)	1904.0(9)
reflns collected	60217	26677	44908	30557	17302
unique reflns	7494	6317	3580	11058	6881
obsrefls [I> 2σ(I)]	4868	4811	2756	6799	3865
R1 [I> 2σ(I)]	0.0834	0.0486	0.0597	0.0838	0.0880
wR2 [I> 2σ(I)]	0.1927	0.1132	0.1229	0.2332	0.1998
CCDC No.	2344979	2344978	2344977	2344981	2344980

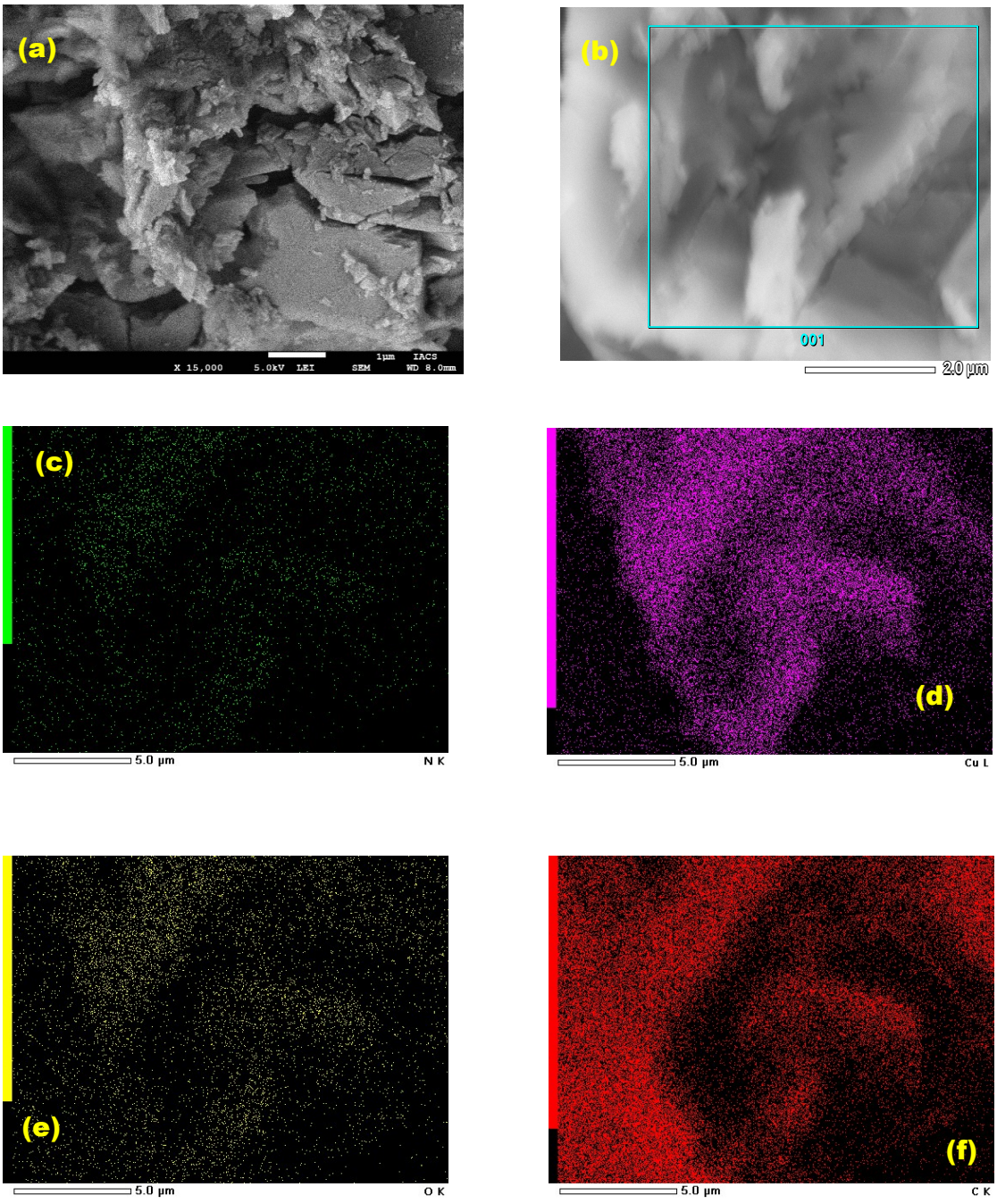

Figure S7 (a) SEM image of MOF-1 showing microscale metal–organic particles, and (b) Focused position of the crystal where EDAX mapping will be carried out. and elemental mapping of MOF-1 showing the elements (c) N, (d) Cu, (e) O, (f) C.

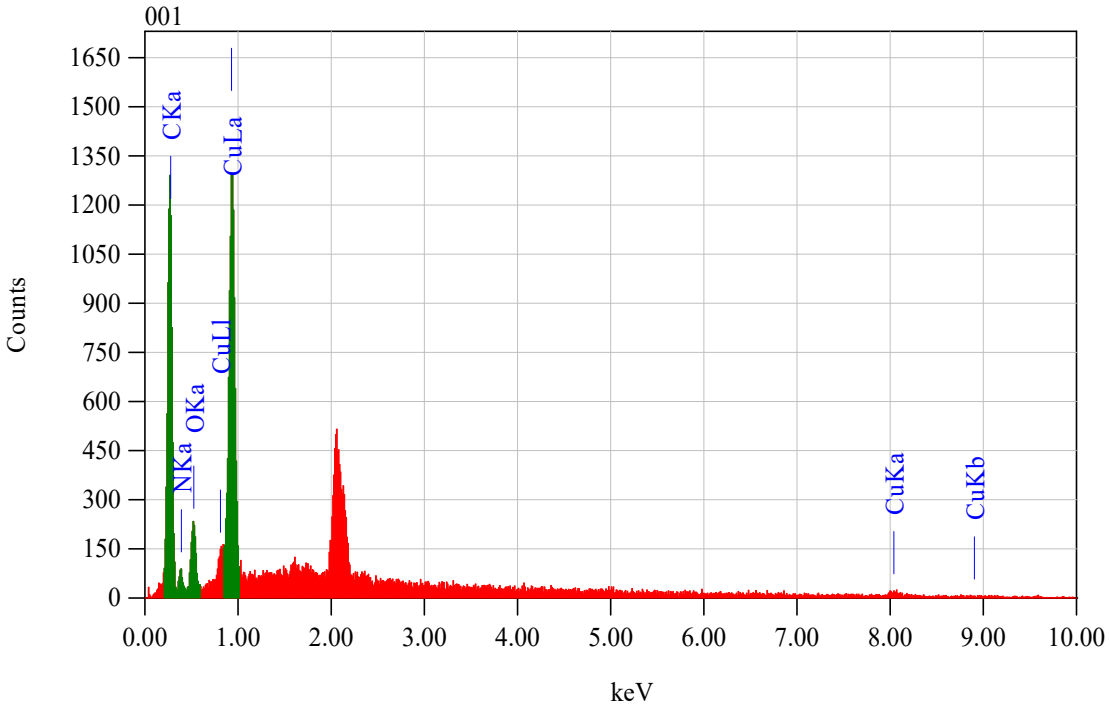

ZAF Method Standardless Quantitative Analysis

Fitting Coefficient: 0.3178

Element	(keV)	Mass%	Sigma	Atom%	Compound	Mass%	Cation	K
C K	0.277	40.23	0.17	68.82				32.4330
N K*	0.392	5.25	0.13	7.70				5.0787
O K	0.525	6.09	0.12	7.82				6.4804
Cu L	0.930	48.43	0.45	15.66				56.0079
Total		100.00		100.00				

Figure S8. % of Counts for each element as constituents in MOF 1.

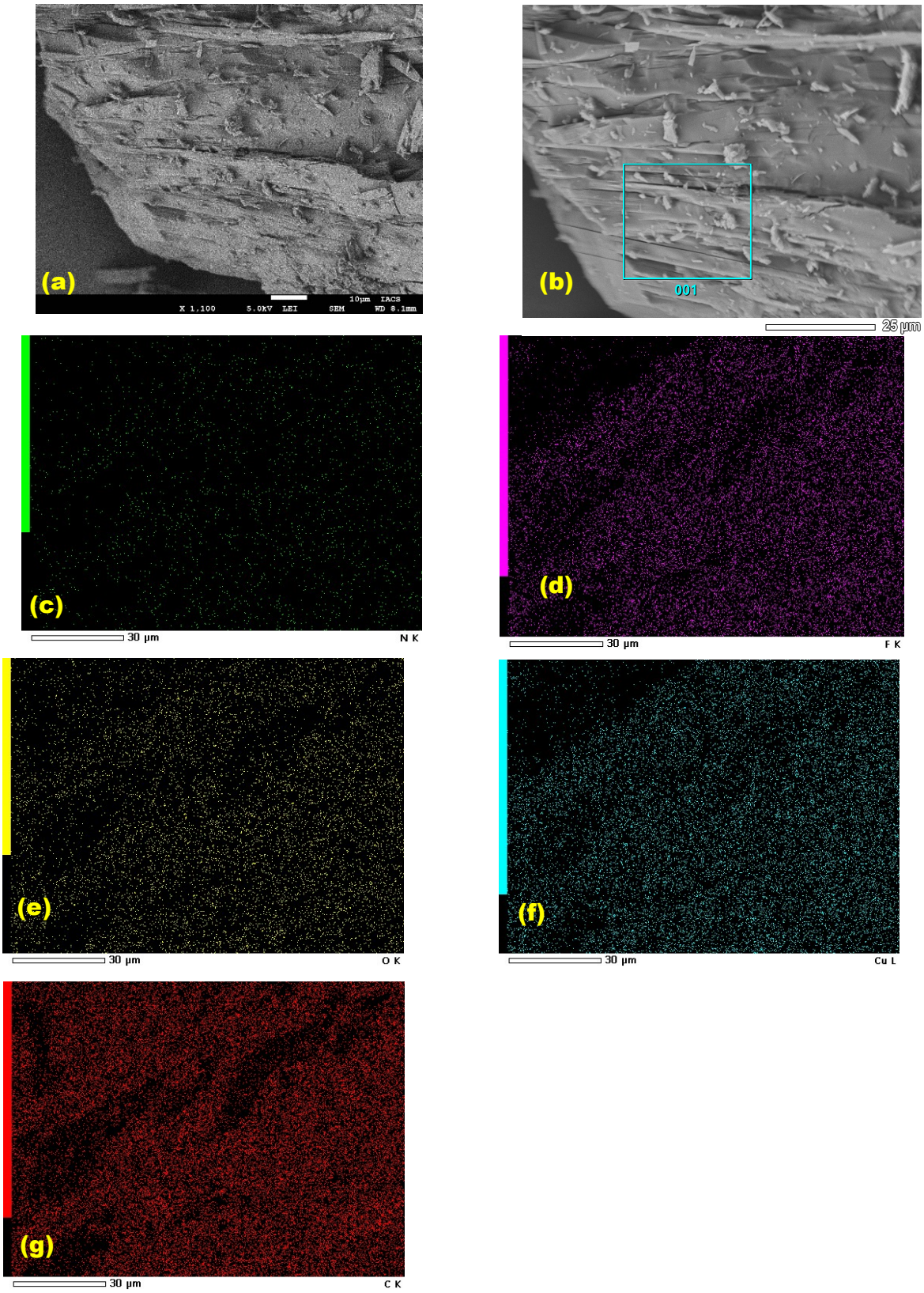

Figure S9. (a) SEM image of MOF-2 showing microscale metal–organic particles, and (b) focused position of the crystal where EDAX mapping will be carried out. and elemental mapping of MOF-2 showing the elements (c) N, (d) F, (e) O, (f) Cu, (g) C.

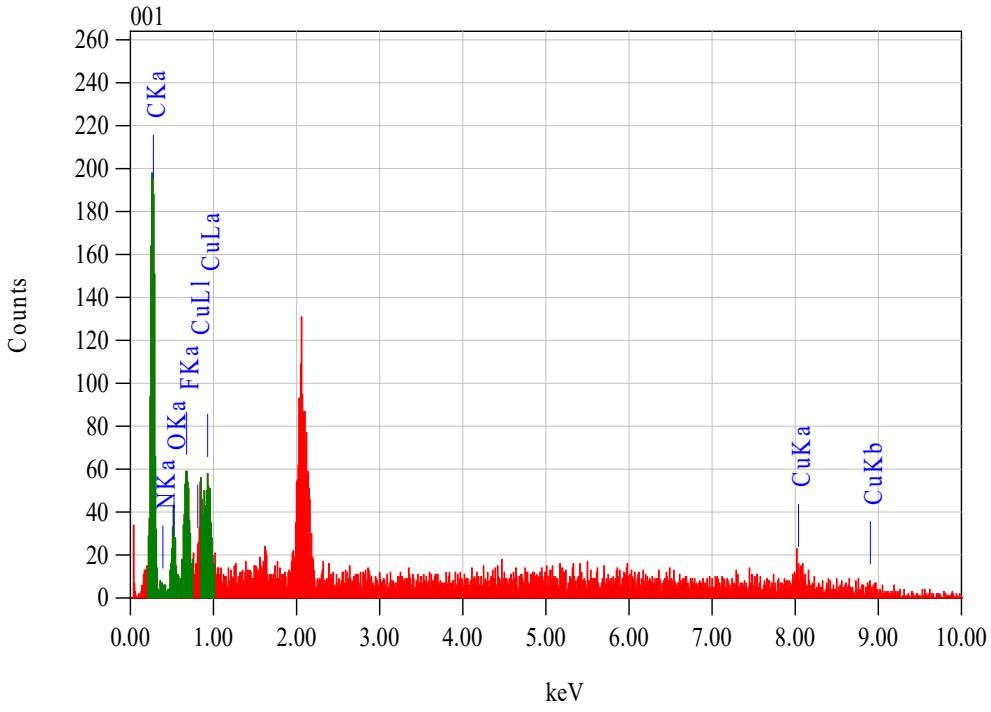

ZAF Method Standardless Quantitative Analysis

Fitting Coefficient : 0.5078

Element	(keV)	Mass%	Sigma	Atom%	Compound	Mass%	Cation	K
C K		0.277	52.36	0.56	65.51			50.4391
N K*		0.392	7.06	0.52	7.58			5.1597
O K*		0.525	10.67	0.56	10.02			9.0257
F K		0.677	17.69	0.78	14.00			25.5934
Cu L*		0.930	12.22	1.29	2.89			9.7822
Total			100.00		100.00			

Figure S10. % of Counts for each element as constituents in MOF 2.

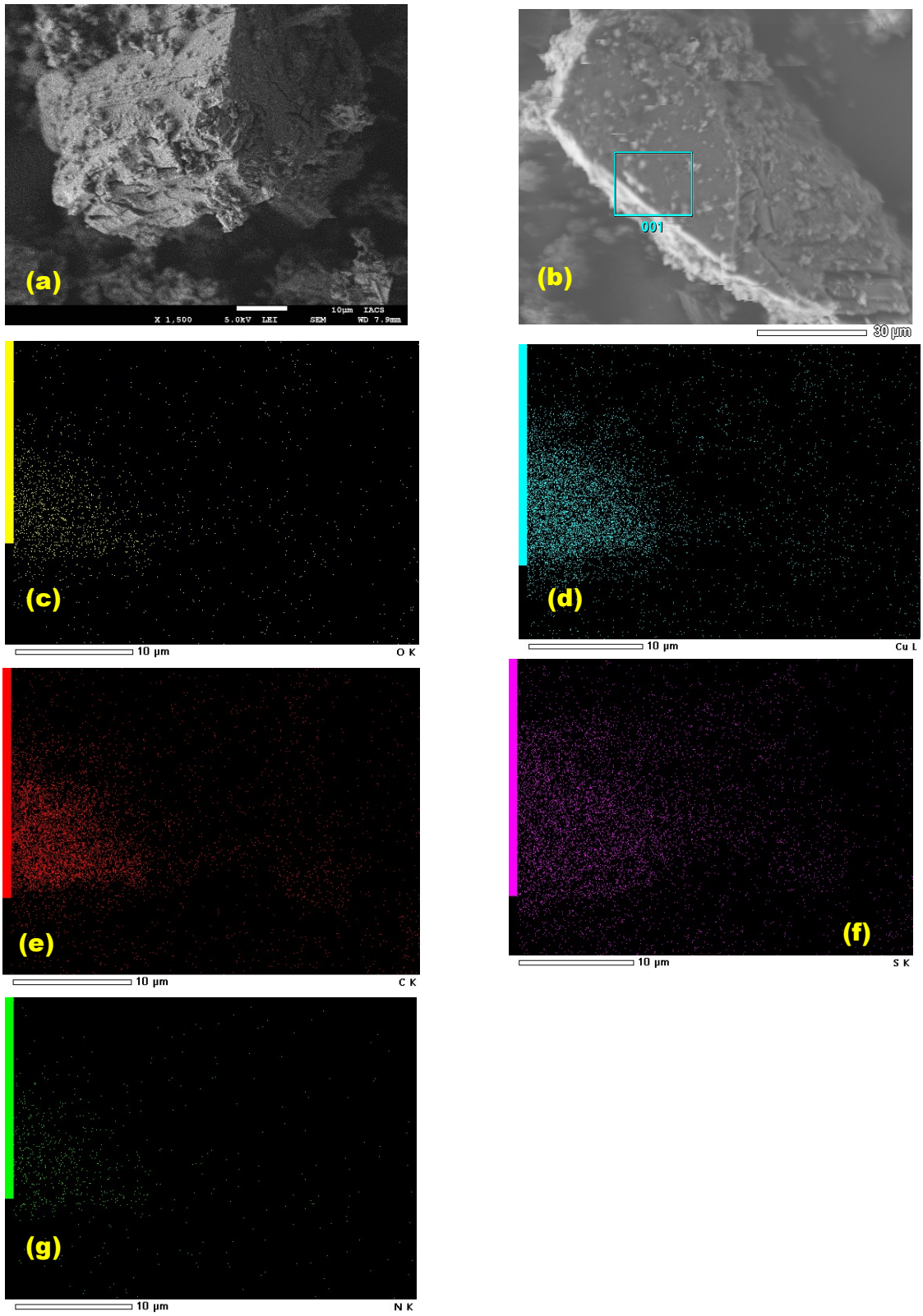

Figure S11. (a) SEM image of MOF-5 showing microscale metal–organic particles, and (b) focused position of the crystal where EDAX mapping will be carried out. and elemental mapping of MOF-2 showing the elements (c) O, (d) Cu, (e) C, (f) S, (g) N.

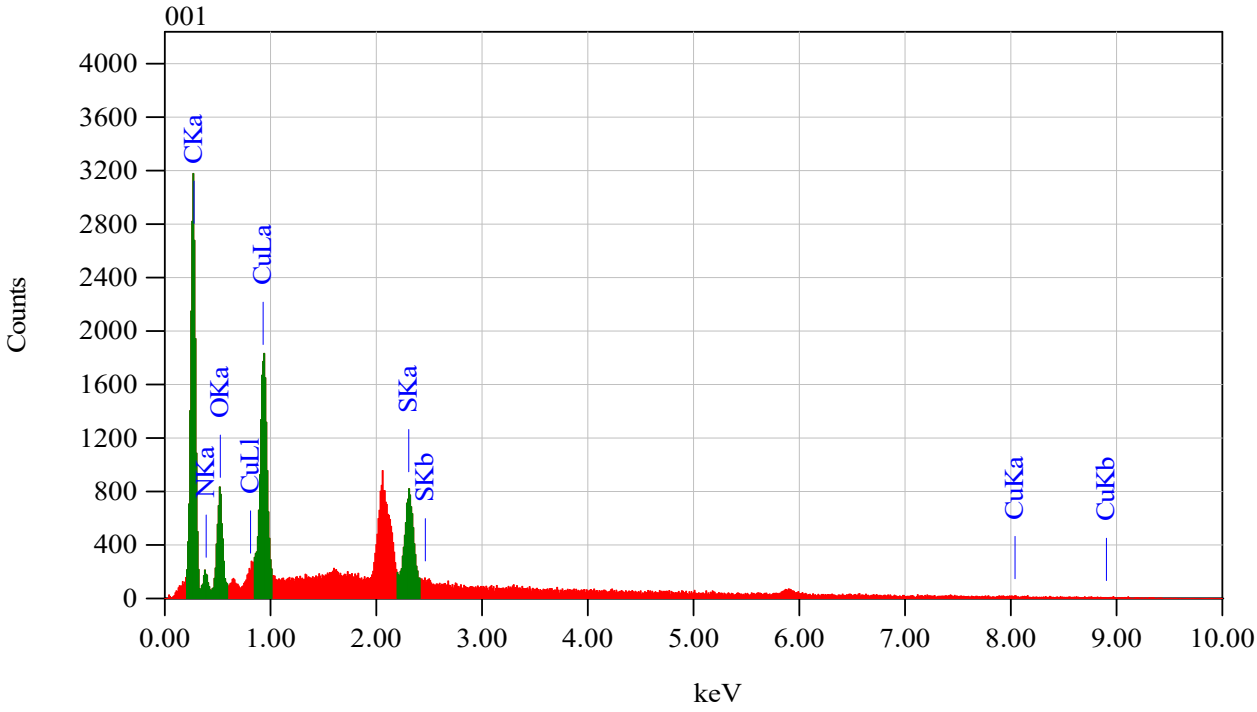

ZAF Method Standardless Quantitative Analysis

Fitting Coefficient: 0.2408

Element	(keV)	Mass%	Sigma	Atom%	Compound	Mass%	Cation	K
C K	0.277	45.49	0.13	69.73				30.0797
N K	0.392	5.81	0.09	7.64				5.1168
O K	0.525	6.43	0.08	7.40				6.6717
S K	2.307	10.52	0.12	6.04				18.8010
Cu L	0.930	31.74	0.22	9.20				39.3308
Total		100.00		100.00				

Figure S12. % of Counts for each element as constituents in MOF 5.

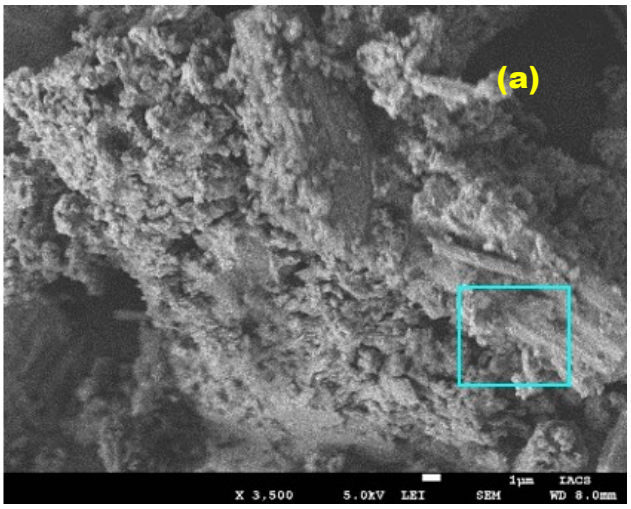

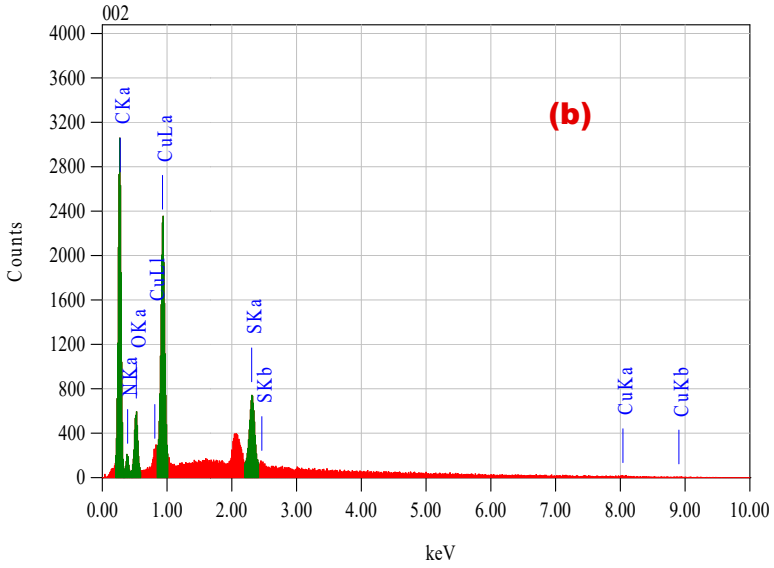

ZAF Method Standardless Quantitative Analysis

Fitting Coefficient: 0.2408

Element	(keV)	Mass%	Sigma	Atom%	Compound	Mass%	Cation	K
C K	0.277	48.49	0.14	59.80				30.0797
N K	0.392	5.11	0.08	8.24				5.1168
O K	0.525	7.34	0.12	6.62				6.6717
S K	2.307	8.52	0.09	5.13				18.8010
Cu L	0.930	30.54	0.20	20.21				39.3308
Total		100.00		100.00				

Figure S13 (a) SEM image of MOF-4 showing microscale metal–organic particles, (b) % of Counts for each element as constituents.

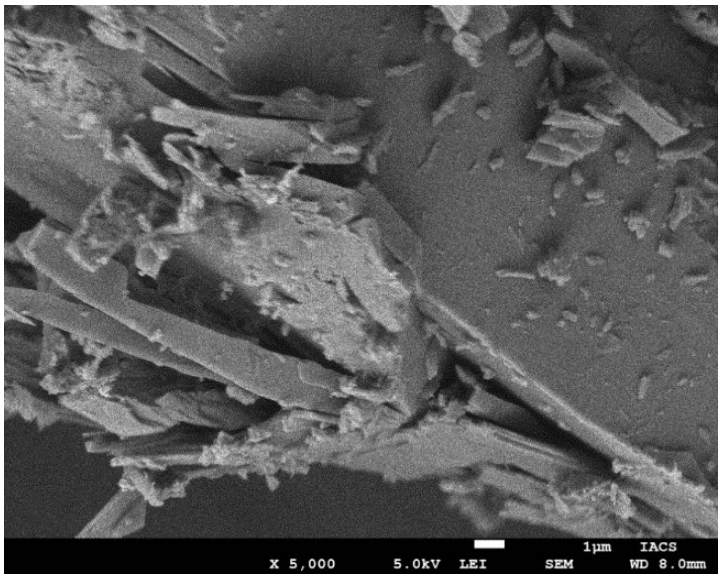

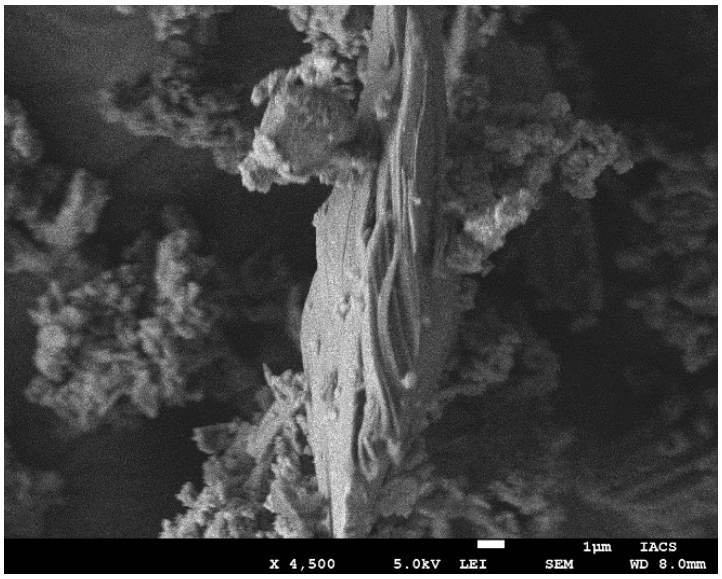

Figure S14. SEM images of MOF-3 showing microscale metal–organic particles.

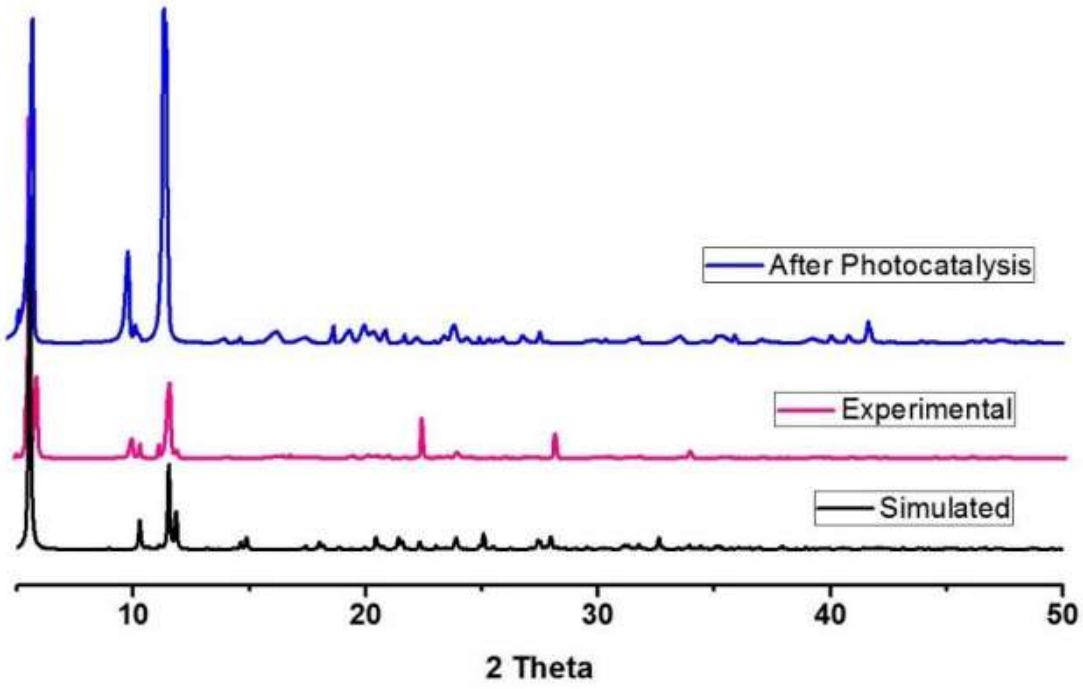

Figure S15: PXRD spectra of MOF-1.

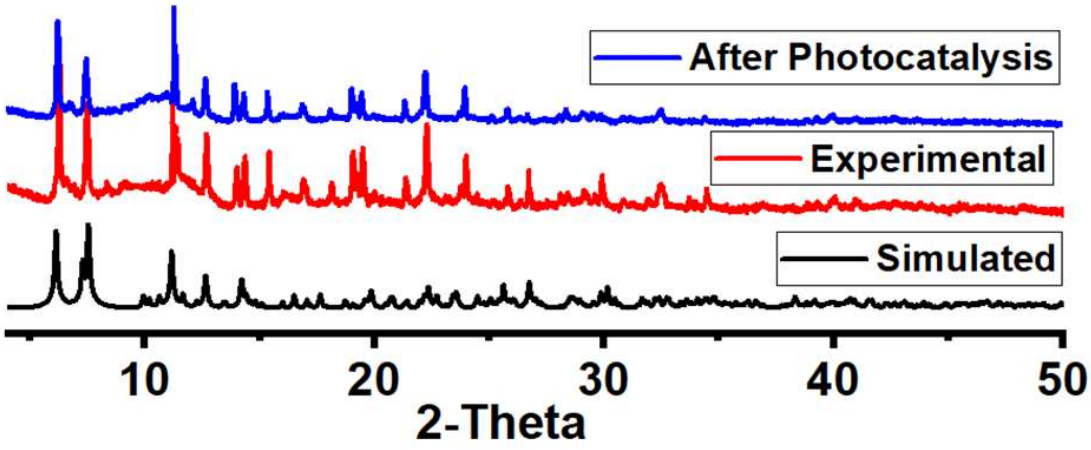

Figure S16: PXRD spectra of MOF-2.

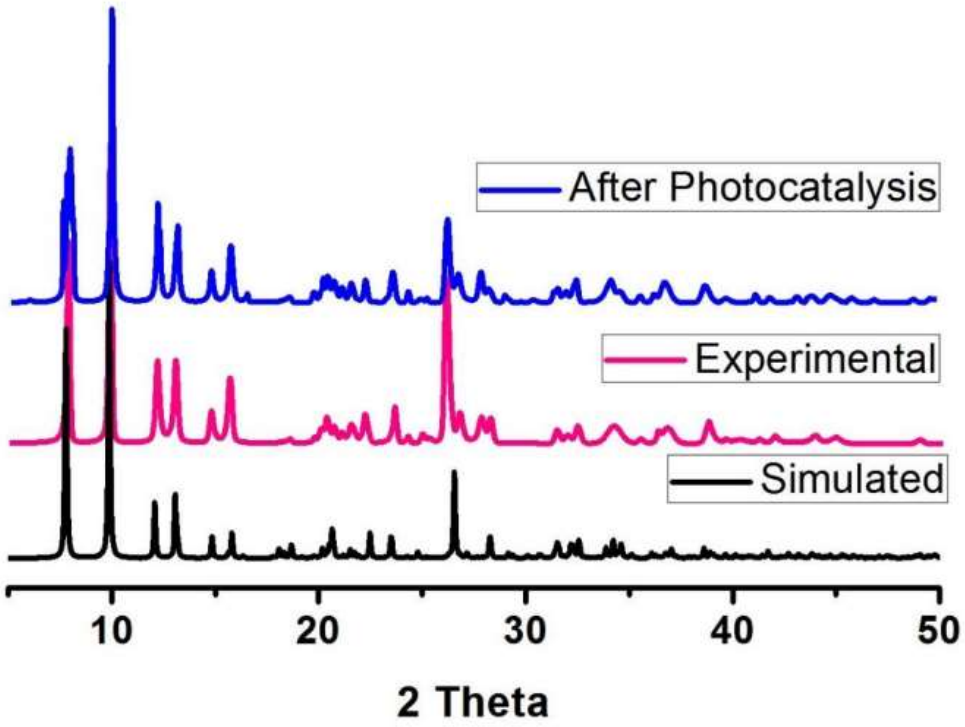

Figure S17: PXRD spectra of MOF-3.

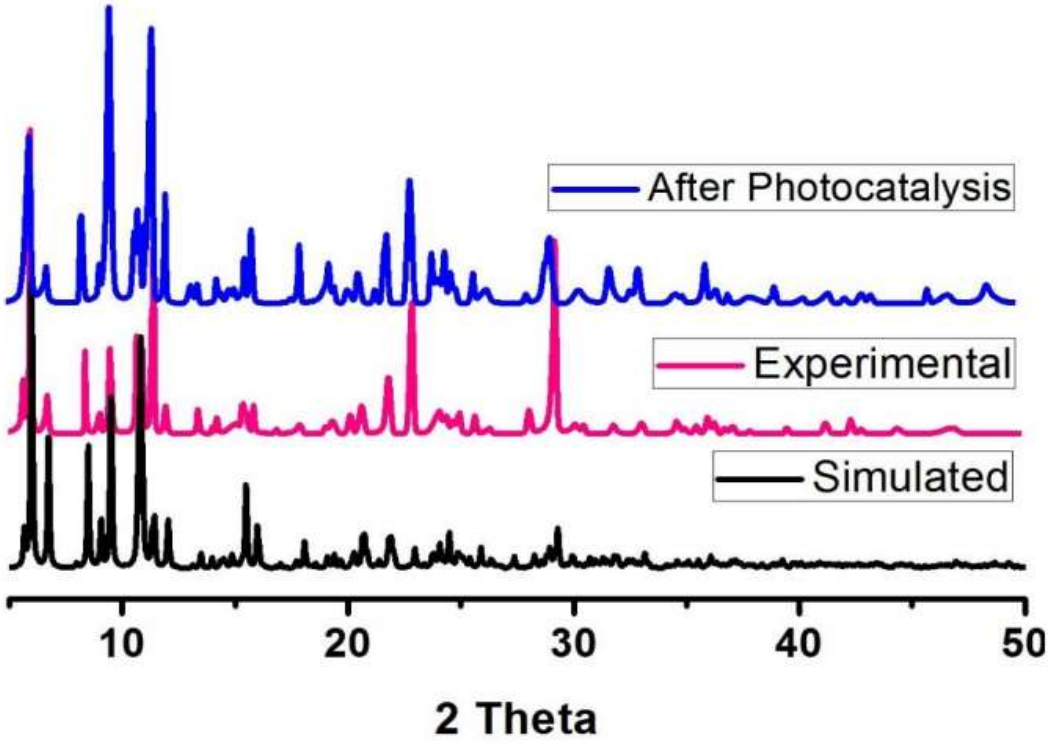

Figure S18: PXRD spectra of MOF-4.

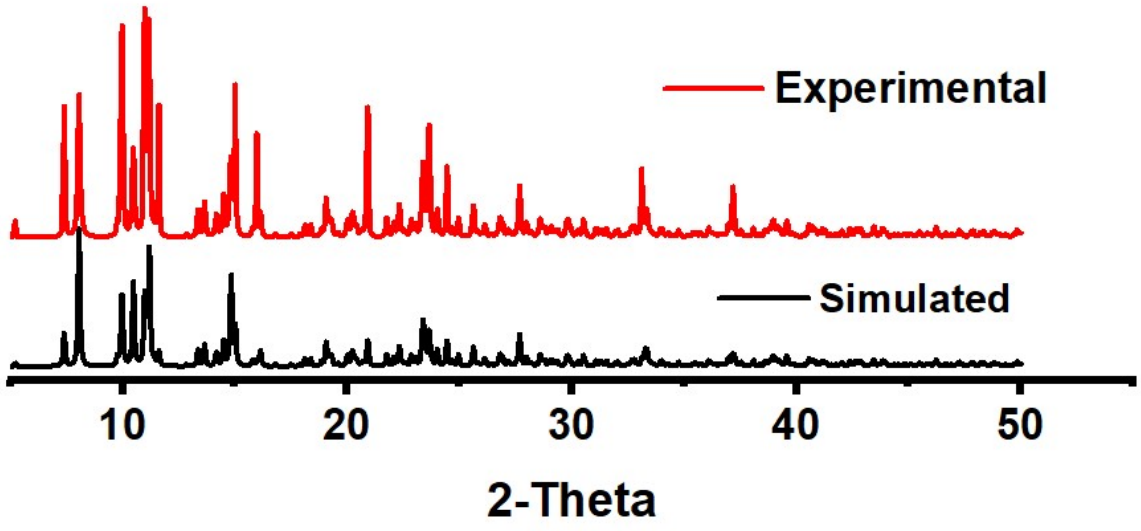

Figure S19: PXRD spectra of MOF-5.

Table S2. Some selected bond lengths (Å) Cu-MOF 1-5.

MOF 1	Cu1 O1 2.003(8)	Cu2 O1 2.004(8)	Cu2 N3 1.947(10)
	Cu1 O2 1.946(9)	Cu2 O3 2.291(10)	Cu3 O1 1.987(8)
	Cu1 N1 1.953(11)	Cu2 O6 1.992(9)	Cu3 O5 1.986(9)
	Cu1 N6 1.944(11)	Cu2 N2 1.947(11)	Cu3 N4 1.950(12)
			Cu3 N5 1.906(12)
MOF 2	Cu1 O1 1.997(3)	Cu2 O1 1.995(3)	Cu3 O4 2.003(4)
	Cu1 O3 2.312(4)	Cu2 O2 1.949(4)	Cu3 N4 1.936(4)
	Cu1 O5 1.970(3)	Cu2 N2 1.947(4)	Cu3 N5 1.940(4)
	Cu1 N1 1.955(4)	Cu2 N3 1.935(5)	Cu3 N7 2.413(7)
	Cu1 N6 1.942(4)	Cu3 O1 2.009(3)	Cu3 O8 2.413(7)
MOF 3	Cu1 O1 2.005(7)	Cu2 N4 1.943(10)	Cu3 N6 1.960(9)
	Cu1 N1 1.943(10)	Cu2 N5 1.945(10)	Cu3 O3A 2.372(17)
	Cu1 N3 1.933(10)	Cu2 O5A 1.951(9)	Cu3 O4A 2.011(13)
	Cu1 O2A 1.92(2)	Cu2 O5B 1.949(9)	Cu3 O3B 2.16(2)
	Cu1 O2B 2.04(3)	Cu3 O1 1.996(7)	Cu3 O4B 2.050(14)
	Cu2 O1 1.991(8)	Cu3 N2 1.952(9)	
MOF 4	Cu1 N1 1.938(7)	Cu3 N1B 1.956(7)	Cu5 N1E 1.939(9)
	Cu1 N2B 1.940(7)	Cu3 N2A 1.969(7)	Cu5 N1F 1.940(9)
	Cu1 O1S 1.984(5)	Cu3 O1S 2.005(5)	Cu5 O3 1.972(6)
	Cu1 O1 1.985(5)	Cu3 N1C 2.029(7)	Cu5 O2S 1.995(6)
	Cu2 N1A 1.945(8)	Cu3 O7 2.336(6)	Cu6 N1G 1.934(7)
	Cu2 N2 1.962(7)	Cu4 N2E 1.927(9)	Cu6 N2F 1.937(8)
	Cu2 O1S 1.988(5)	Cu4 N2G 1.936(8)	Cu6 O2S 1.998(7)
	Cu2 N1D 1.997(7)	Cu4 N1H 2.008(9)	Cu6 N1I 2.020(9)
	Cu2 O5 2.344(5)	Cu4 O2S 2.029(6)	Cu6 O4 2.373(8)
MOF 5	Cu01 N00B 1.918(7)	Cu02 O00A 1.951(7)	Cu03 N00E 1.958(8)
	Cu01 N00F 1.933(8)	Cu02 N00D 1.977(8)	Cu03 N00N 1.980(9)
	Cu01 O006 1.952(6)	Cu02 O005 1.998(6)	Cu03 O005 1.999(6)
	Cu01 O005 1.984(6)	Cu02 O00G 2.380(8)	Cu03 O008 2.388(7)
	Cu02 N00H 1.942(8)	Cu03 N00M 1.938(8)	

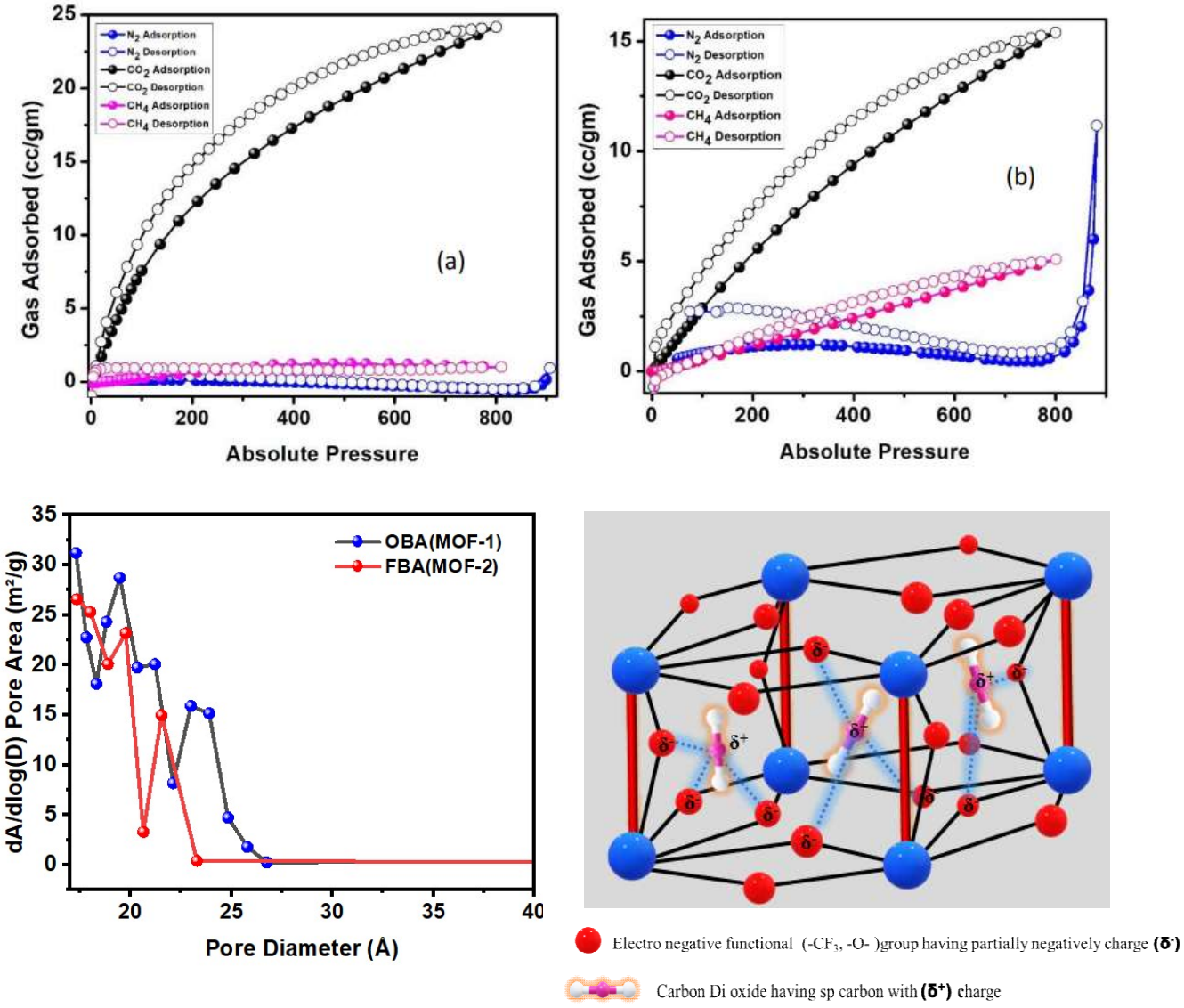

Figure S20: Typical type I gas adsorption isotherms of (a) MOF-1 and (b) MOF-2 showing selective CO_2 gas sorption (black circles) over N_2 (blue circles) and CH4 (pink circles) at 273 K. The filled and open circles represent adsorption and desorption, respectively.(c) Pore Size analysis of MOF-1 and MOF-2.(d) Schematic representation of interaction between the functional group and CO_2 molecule presentsin the pore's surface of the MOFs.

Gas Adsorption Studies: The porous network alongside the solvent filled channels led us to explore the physisorptionproperties of the compounds. The presence of different functional groups in the moietyprompted us to investigate the selective gas sorption capabilities. It is well known fact thatMOFs having O, F, S etc in the functional groups have shown great selectivity in adsorbingcarbon dioxide selectively. Before proceeding the experiments trapped solvent molecules mustbe removed or exchanged by low boiling solvent molecules. To achieve that the samples weredipped into a mixture of methanol and DCM (1/1) solutions, stirred for a while and finally kept undisturbed for 12 hours.The process of solvent exchange was repeated for 3 times before drying it to 120°C undervacuum. The nitrogen sorption studies were done at 77K under the pressure range of 0-1atmwhereas CO_2 and CH_4 adsorption studies were carried out at 273 under the same pressure range.All the MOFs showed very poor uptake for nitrogen and methane, however, it was interestingto note that **MOF-1** and **MOF-2** have showed selective adsorption affinity towards CO2 gas. As it can be seen in above figure MOF**1** adsorbed around 25 cc/gm CO2 and **MOF-2**adsorbed 15cc/gm whereas the amount of nitrogen and methane adsorbed by **MOF-1** isalmost negligible and for **MOF-2** its merely around 12cc/gm and 5cc/gm respectively.The corresponding pore diameters distribution for **MOF 1** and **MOF 2** are 17-27.5Å and 17-23Å accordingly based on N_2 gas adsorption data.We have also calculated the surface are for **MOF 1** and **MOF 2.** For **MOF 1**BET Surface Area: 1.4812 $m^2/g$and for **MOF 2** BET Surface Area: 4.1861 m^2/g based on N_2 gas adsorption data.The **MOF 1**, **MOF 2** has the most electro negative functional groups **(-CF_3, -O-)** present which are free and faced towards the pore of the MOF. As a result because of their electronegative property the **δ-** charge separation occurs throughout the pore surface of the MOF. CO_2 has a sp-carbon atom in its centre having **δ+** charge resulting a very strong coulombic interaction between the functional group and guest moiety so all though the adsorption of neutral N_2 gas molecule is poor by the MOFs the same thing occurs for the methane also but they show significantly high adsorption for the CO_2 gas in room temperature.

Photocatalytic degradation of toxic organic

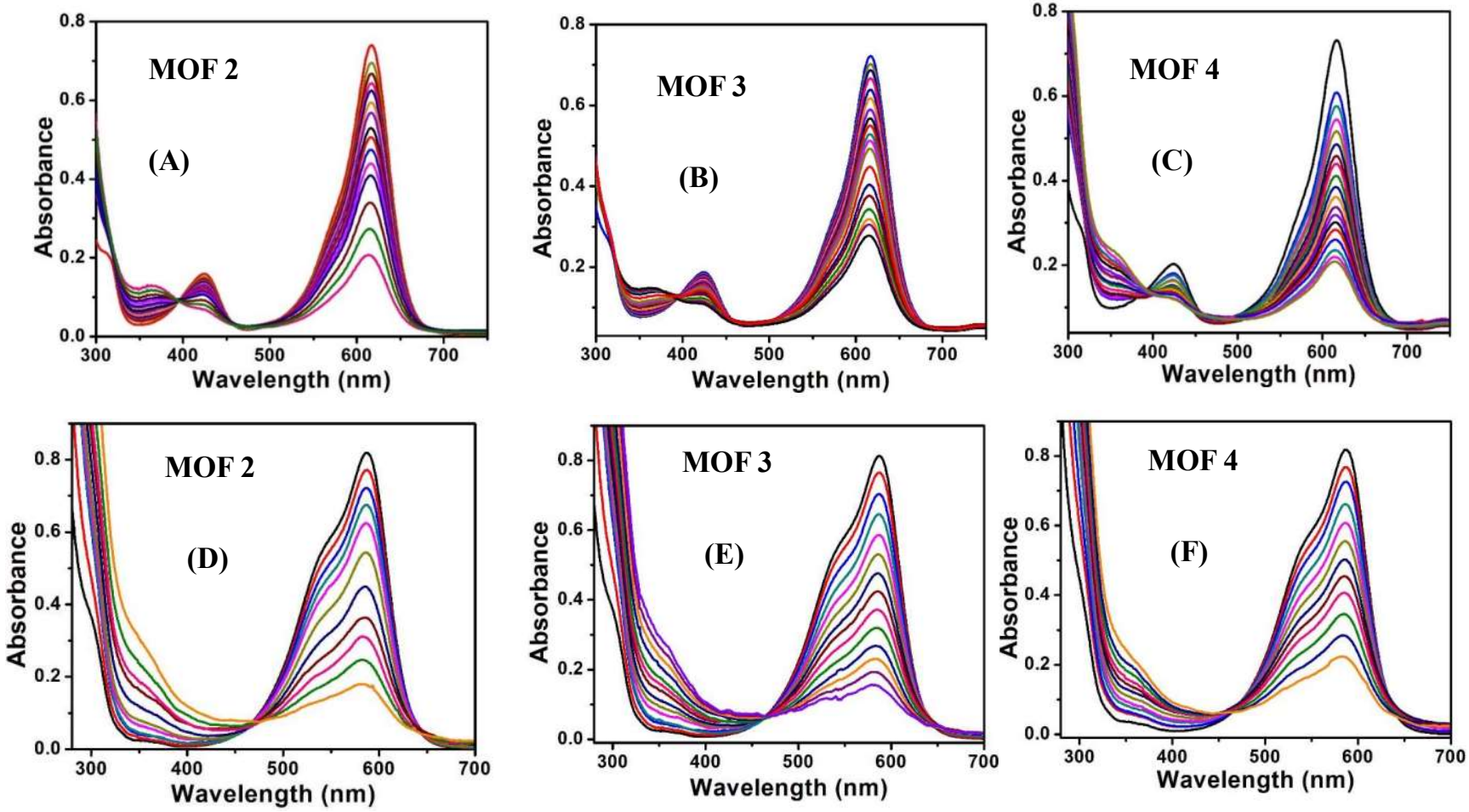

Figure S21. Change of absorption spectra of the solution of (a)-(c) malachite green dye solution and (d)-(f) crystal violet dye solution in presence of MOFs 2- 4 under exposure of UV light at room temperature.

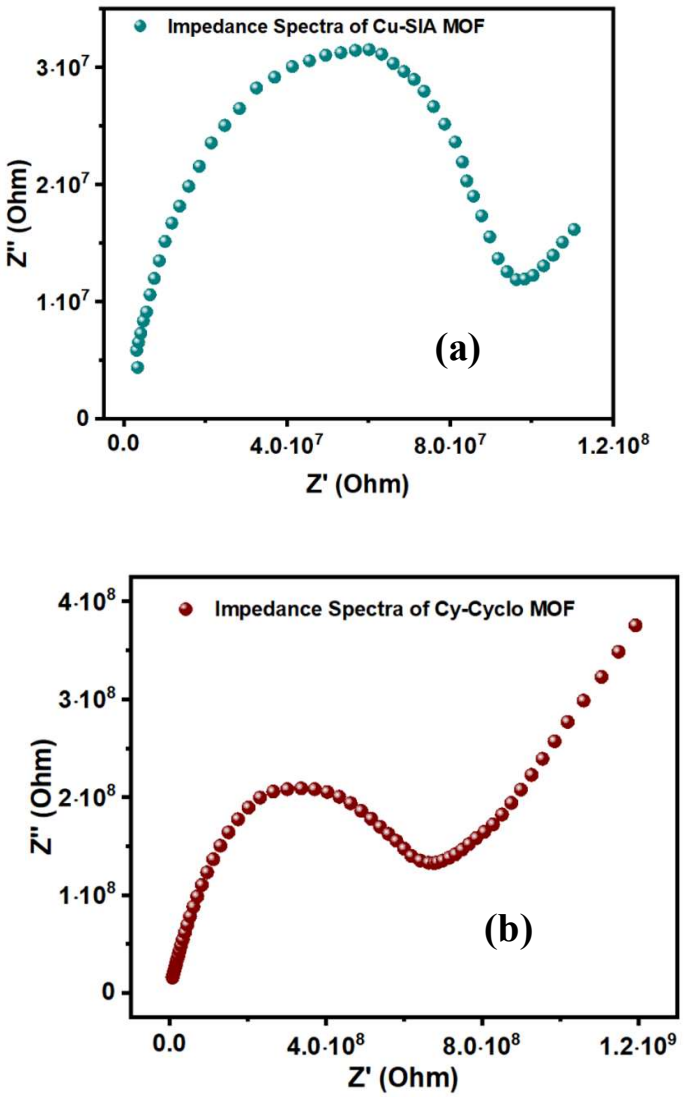

Figure S22. Impedance spectra of (a) Cu-SIA and (b) Cu-CYO MOF.

Table S3. Proton conductivity data for the MOFs 1-5.

Sample Name	Relative Humidity	Temperature	Conductivity
MOF 1	95%	30°C	$1.06*10^{-6}$ S/cm
		45°C	$1.32*10^{-6}$ S/cm
		60°C	$2.46*10^{-6}$ S/cm
		70°C	$2.90*10^{-6}$ S/cm
		80°C	$3.54*10^{-6}$ S/cm
MOF 2	95%	30°C	$7.39*10^{-7}$ S/cm
		45°C	$9.11*10^{-7}$ S/cm
		60°C	$1.30*10^{-6}$ S/cm
		70°C	$2.12*10^{-6}$ S/cm
		80°C	$8.94*10^{-6}$ S/cm
MOF 3	95%	80°C	$6.72*10^{-11}$ S/cm
MOF 4	95%	80°C	$1.24*10^{-10}$ S/cm
MOF 5	95%	30°C	$1.43*10^{-6}$ S/cm
		45°C	$1.88*10^{-6}$ S/cm
		60°C	$2.69*10^{-6}$ S/cm
		70°C	$4.61*10^{-6}$ S/cm
		80°C	$8.91*10^{-6}$ S/cm

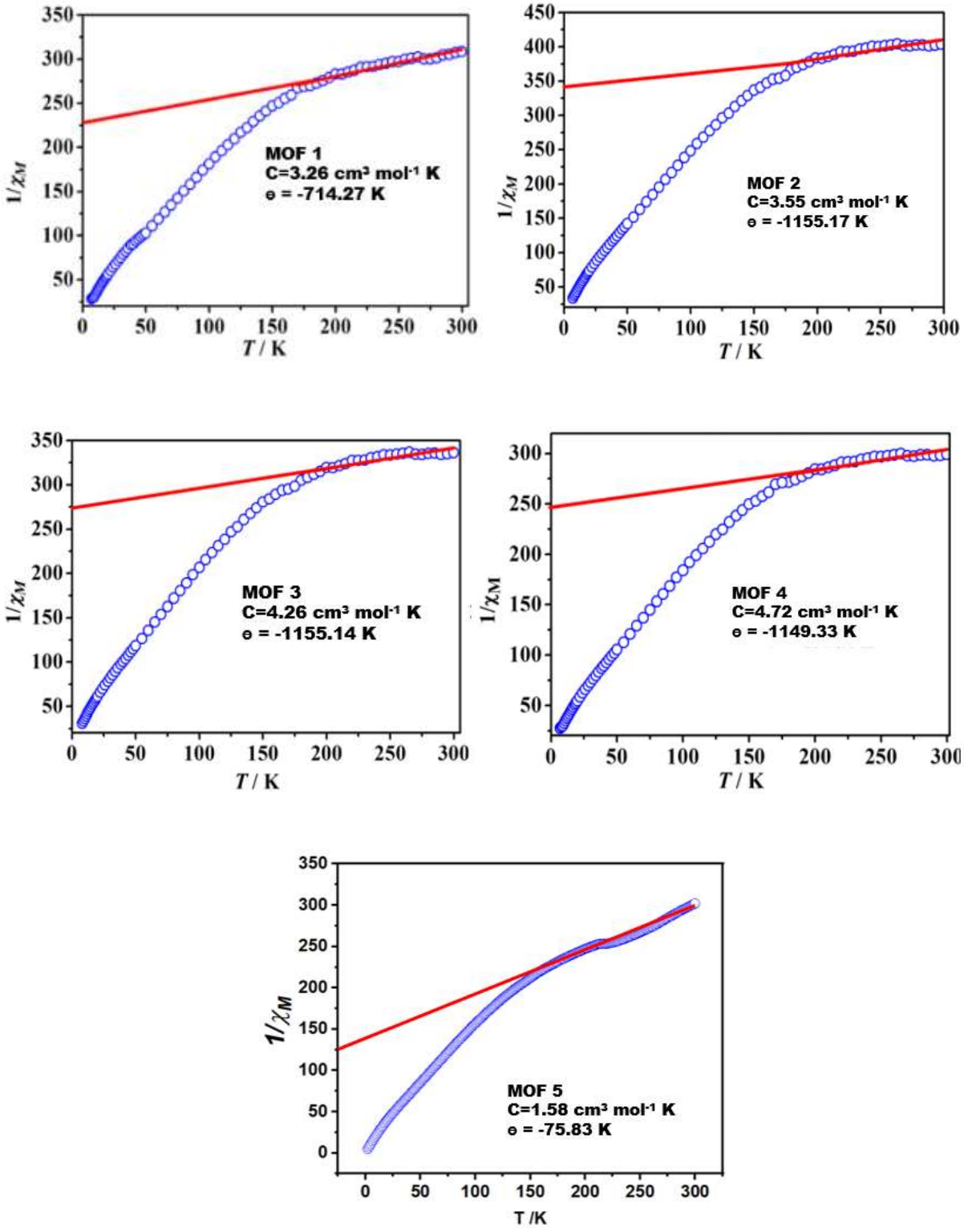

Figure S23. (a)-(e) Temperature dependence of 1/χM vs T plot for MOFs 1-5 in the temperature range of 2−300 K under an applied field of 1000 Oe. The red lines indicate the best fit obtained from the Curie−Weiss equation at higher range of temperature.

Table S4. Comparison of dye degradation by MOF in aqueous conditions by some previously reported MOFs

MOF Catalyst	Dye	Efficiency (%)	Time (min)	k (min^{-1})	Ref.
$Co_3(BPT)_2(bpp)$	RhB	90	120	0.0192	RSC Adv., 2018, 8, 36400-36406
MIL-53(Fe)	RhB	98	40	0.0794	Appl. Catal.B, 2014, 148-149, 191-200
$[Co(bpba)(bdc)_{1/2}]$	MB	84	180	-	J.Mater. Chem. A., 2015, 3, 6962-6969.
Cd-PDA	MB	85	120	0.0153	J. Mater. Chem., A, 2016, 4,16349-16355.
$[Co_2(1,4\text{-BDC})(NCP)_2]$	RhB	68	300	-	Inorg.Chem. Commun., 2013, 35, 130-134.
$[Co_2(1,4\text{-BDC})(NCP)_2]$	MB	63	300	-	Inorg.Chem. Commun., 2013, 35, 130-134.
$[Zn_3(BTC)_2(H_2O)_3]$	MB	79	90	0.0084	Cryst. Growth Des. 2020, 20, 12, 7833–7839.
MOF-2	MB	77.89	80	0.0188	Cryst. Growth Des. 2019, 19, 2, 992–1004
MOF-3	CR	71.25	80	0.0202	Cryst. Growth Des. 2019, 19, 2, 992–1004
$\{[Co_2(dmphen)_2(CPCA)_2]\ DMF\}_n$	MB	98	35	0.0080	ACS Omega 2018, 3, 11, 15315–15324
MOF-1	MG	62.31	80	62.31	This work
MOF-2		71.86	80	71.86	
MOF-3		77.08	80	77.08	
MOF-4		61.72	80	61.72	
MOF-1	CV	72.84	80	72.84	This work
MOF-2		78.19	80	78.19	
MOF-3		73.87	80	73.87	
MOF-4		80.76	80	80.76	

Rh-B: Rhodamine-B; MB: Methylene Blue; MG: Malachite Green; CV: Crystal Violet; CR: Congo Red.

Table S5. Comparison of the proton conductivities of MOFs with other proton-conducting materials.

Materials	Conductivity ($S\ cm^{-1}$)	Testing conditions	Ref.
Mg−(p-H6L)	9.75×10^{-5}	41 °C and 98% RH	Inorg.Chem. 2013, 52, 8770-8783.
$[Zn_5(o\text{-}CPhH_2IDC)_2(o\text{-}CPhHIDC)_2(2.2'\text{-}bipy)_5]n{\cdot}5H_2O$	5.00×10^{-5}	100 °C and 100% RH	Chem.Commun. 2014, 50 (15), 1912-1914.
$\{[Zn(C_{10}H_2O_8)_{0.5}(C_{10}S_2N_2H_8)]{\cdot}5H_2O]\}n$	2.55×10^{-7}	80 °C and 95% RH	J. Am.Chem. Soc. 2011, 133, 17950-17958.
$\{[Zn(2,6\text{-}ndc)\ (aldrithiol)]{\cdot}3(H_2O)\}n$	6.73×10^{-7}	45 °C and 95% RH	J. Solid StateChem. 2015, 229, 103-111
$[Cu_4(HDMPhIDC)_4(H_2O)_4]n$	2.58×10^{-5}	100 °C and 98% RH	Chem. Eur. J. 2019, 25(62), 14108-14116.
$[Mn(oCPhH_2IDC)(4.4'bipy)0.5(H_2O)_2]n{\cdot}3H_2O$	5.74×10^{-5}	100 °C and 98% RH	Chem.Commun. 2014, 50 (15), 1912-1914.
$[Ni_3(HL)_2(H_2O)_{10}]{\cdot}4H_2O$	1.43×10^{-3}	4 °C and 100% RH	New J. Chem. 2019, 43, 807-812.
MOF 1	$3.54*10^{-6}$ S/cm	80 °C and 95% RH	ThisWork
MOF 2	$8.94*10^{-6}$ S/cm	80 °C and 95% RH	
MOF 5	$8.91*10^{-6}$ S/cm	80 °C and 95% RH	